We are IntechOpen, the world's leading publisher of Open Access books Built by scientists, for scientists

6,900
Open access books available

186,000
International authors and editors

200M
Downloads

154
Countries delivered to

Our authors are among the

TOP 1%
most cited scientists

12.2%
Contributors from top 500 universities

WEB OF SCIENCE™

Selection of our books indexed in the Book Citation Index
in Web of Science™ Core Collection (BKCI)

Interested in publishing with us?
Contact book.department@intechopen.com

From Optical Acquisition to Rapid Prototyping: Applications to Medicine and to Cultural Heritage

Giovanna Sansoni and Franco Docchio
Optolab, Laboratory of Optoelectronics, University of Brescia
Italy

1. Introduction

In addition to CAD techniques currently used to produce a 3D model of an artifact for subsequent prototyping, 3D acquisition by means of optical digitizers is dramatically growing as a powerful companion of rapid prototyping, for the creation of prototypes from existing objects such as maquettes, sculptures and body parts. The availability of a large amount of 3D acquisition systems on the market, both based on lasers and on incoherent light, greatly facilitates the process. In general terms, a reconstruction process is based on the steps of (i) acquisition, (ii) point cloud elaboration, (iii) mesh generation, (iv) STL (or equivalent) file generation, and finally (v) prototyping.

Our Laboratory has been involved for years in the development and use of 3D scanners. The aim of this chapter is to illustrate the pathway from the object under interest to the prototype. We will present the main results of the research carried out in the fields of maxillofacial reconstruction, forensic medicine and cultural heritage, using optical 3D range sensors (3DS), reverse engineering (RE) and rapid prototyping (RP) techniques.

The first activity originated from a request of our University dentistry specialists, in 2007. The aim was to develop the procedure for producing facial prosthetic elements able to reduce the patient's discomfort and the dependence on the anaplasthologist skill, and to increase the process efficiency and performance.

The second activity originated from a request of the Italian State Police in 2004. The goal was to assess the feasibility of using contactless sensors to (i) document crime scenes before their removal, and (ii) measure lesions on cadavers in post mortem analysis.

The third activity has been carried out since 2001 upon request of archaeologists interested in studying, monitoring and reproducing pieces of cultural interest.

Over the years, we have accumulated a remarkable experience in these fields. On one hand, we have been helped by the experience previously accumulated at the Laboratory in the frame of 3DS, RE and RP, especially in applications typical of mechanical, manufacturing and automotive industry (Sansoni & Docchio, 2004; Sansoni & Docchio, 2005). On the other hand, we were excited by the opportunity of exploiting our experience even in fields far from industrial production, such as those mentioned above.

Although 3DS, RE and RP methods are well known in production fields, their experimentation in the applications of interest here is recent. In maxillo-facial prosthetic

reconstruction, Computer Tomography (CT) and Magnetic Resonance Imaging (MRI) systems have been proposed for the prosthetic restoration of facial defects (Jiao et al., 2004). They represent a significant evolution with respect to traditional techniques, since the contact with the patient's face is avoided, and a very detailed description of tissues and shapes is achieved (Taylor, 2000). However, they are very invasive and expensive.

Only recently the use of 3D optical sensors and Rapid Prototyping have been proposed to safely acquire patient's face parts for modeling and reproducing prosthetic elements (Tsuji et al., 2004). This trend is justified by (i) their non invasiveness for the patient, due to the pure-reflective approach to the measurement, (ii) their acquisition speed, which increases the patient comfort and guarantees measurement accuracy even with unavoidable patient movements, (iii) their market availability at by far lower costs with respect to CT/MRI systems, and (iv) their performances in terms of data quality, system portability and ruggedness.

As far as forensics is concerned, the literature has pointed out the use of radio-diagnostic tests, such as scanning electron microscopy (SEM), MRI and CT, to improve the quality of detail on the shape and size of tools in bone lesions (Thali et al., 2003). In addition, bite marks analysis has been approached using photogrammetry (Thali et al., 2000). The use of pure reflective 3D optical sensors has only recently been published in forensics, for example to verify the consistency of a wound morphology with the injury tool used (Bruschweiler et al., 2003).

The interest in investigating the potential offered by optical digitizers has grown over the years, mainly because (i) the analysis is faster than with 3D SEM and CT, (ii) they exhibit very good measurement performances in the macroscopic range, and (iii) they are designed to measure in harsh conditions. Optical digitizers are rugged and portable, and can be used on-site (i.e., directly on the crime scene and to analyse the victim in short times). In addition, very powerful analysis software is now available to produce models suitable for rapid prototyping fabrication of body segments, in view of subsequent analysis.

The application to cultural heritage is another field where a well-performed set of measurements on a computer-resident replica of the piece, obtained in turn from a high accuracy 3D digitization of the original artwork, would greatly help specialists to perform their analysis. In fact, measurements are still today performed by means of calipers and compasses. This work is time-consuming, invasive (the compass's tips touch and scratch the surface), uncomfortable, and particularly difficult in the case when a distance between non-adjacent locations must be measured. Gross errors usually derive from the intrinsic uncertainty of the measurement, and from the somewhat subjective placement of the fiduciary points between different scientists.

It is now clear that the reproduction (either virtual or physical) of monuments, buildings, statues, ancient handicrafts and archaeological findings would open the door to many applications. They are (i) the remote study of the pieces of interest from a common and reliable data base, (ii) the timely monitoring of the degradation of the pieces in view of a possible restoration, (iii) the visualization of the pieces to fully exploit the concept of "virtual museums", (iv) the production of accurate replicas of the pieces by means of Rapid Prototyping tools, and (v) the storage of digitized 3D images for the creation of 3-D archives (Boulanger et al., 1998).

This chapter is composed as follows. Section 2 describes the application to maxillofacial reconstruction, with reference to two study cases. The former deals with the production of a nose replica, the latter with the production of an ear.

Section 3 presents an example of the work performed in forensiscs, and deals with the prototyping of a skull. Section 4 is dedicated to heritage applications, and details the work performed to build the physical models of a statue.

2. The application to maxillofacial reconstruction

An interesting field of application of rapid prototyping is represented by the development of prostheses in post oncological reconstruction and in congenital defect treatment of the human face. Both functional and aesthetic characteristics of the prosthesis are crucial to allow patients to overcome social, psychological and economic problems deriving from their handicap.

Traditional techniques require the use of impression making procedures and the manual sculpturing of the prosthesis (Brasier, 1954; Roberts, 1971). These procedures present a number of lacks. Firstly, impression making results in patient's discomfort and stress. In addition, the pressure that must be applied on the face to guarantee the required quality of the impression results in the deformation of soft tissues, and in the impossibility of acquiring the original face features and look. Secondly, the quality of the wax positive replica is dependent on the artistic skills of an experienced anaplasthologist. The performance of the process strongly depends on both shape and extension of the defect. Human error contribution, subjectivity in the reconstruction, low reproducibility of the process, and poor initial shape information often lead to serious unfitting of the final prosthesis, under both functional and aesthetic viewpoints. Thirdly, the mould production process is cumbersome and time consuming. The overall process is not adaptive: whenever the existing prosthesis must be replaced, the overall process must be carried out from scratch.

Our activity was aimed at developing a fabrication process able to overcome these limitations. The clinical cases taken into consideration belong to two main categories: (i) the missing anatomic part is unique, as in the case of a nose; (ii) the contralateral organ is available, and it can be used as reference after mirroring, as in the case of an ear.

2.1 The optical digitizer

In the experiments we used the Vivid 910 laser digitizer (Konica Minolta, Inc), shown in Fig. 1. The principle of measurement is based on laser triangulation (Blais, 2004). A plane of laser light from the Vivid's source aperture scans the object. This plane of light is swept across the field of view by a mirror, rotated by a precise galvanometer. The laser light is reflected from the surface of the scanned object. Each scan line is observed by a single frame, and captured by the CCD camera. The contour of the surface is derived from the shape of the image of each reflected scan line. The entire area is captured in 8 seconds (0.3 seconds in FAST mode). A brilliant (24-bit) color image is captured at the same time by the same CCD. The system is rugged, portable, and extremely compact. It can be mounted on a tripod and properly oriented into the measurement volume to optimize the acquisition viewpoint. It is equipped with three lenses, having WIDE (8mm), MIDDLE (14mm) and TELE (25mm) focal lengths. They increase the range of variability of the measurement parameters and allow the system to easily adapt to the acquisition problem. Typical values of the measurement parameters are listed in Table 1.

2.2 The elaboration process of 3D data

The process of measurement and data elaboration consists of the following tasks:

1. The acquisition of the point clouds. To accomplish the digitization of complex scenarios it is necessary to perform multiple acquisitions from different point of views and with different degrees of detail.
2. The multi-view registration. It consists of the alignment of the set of the captured point clouds into a common reference frame. The module *ImAlign*, from the Polyworks suite of programs (InnovMetric, Ca, USA) accomplishes this task.
3. The creation of the triangle-mesh. The 3D data of the point cloud are merged into a model that includes information about the topological contiguity of the points. This phase is performed by the use of *ImMerge* module of Polyworks.
4. The editing of the triangle mesh. The model is elaborated to (i) decrease noise influence, (ii) measure point-to-point distances, sections and areas, (iii) render the 3D representation for further VMRL interaction, and (iv) topologically control the model for prototyping applications. This phase is performed by using the *ImEdit* module of Polyworks.
5. The elaboration of STL format files for the production of physical copies of the surfaces by means of rapid prototyping techniques.

Focal lengths	FOV (mm²)	WD (mm)	Zrange (mm)	Rz (mm)
Wide	1000x1000	2000	1000	0.65
Middle	600x450	1000	500	0.3
Tele	140x100	600	200	0.13

Table 1. Typical values of the measurement parameters of the Vivid 910 device. FOV: Field of View, WD: Working Distance, Zrange: Range of measurement, Rz: Measurement resolution

Fig. 1. The optical digitizer Minolta Vivid 910 (left); example of stripe deformation (right)

2.3 Nose reconstruction

Nose reconstruction is a hard problem, since there is no contralateral organ that can be used as a template to reproduce the lost part. In the traditional procedure, a wax model of the nose is manually sculptured 'from scratch' and manually tried-in onto the patient's face, to refine its shapes until sufficient adherence of the prosthesis to the face tissues is achieved.

The quality of the final result depends on sculptor ability, involves patient's discomfort and is seldom aesthetically pleasant.

In our study, we focused onto two main objectives. The former was to reduce the try-in of the prosthetic element, the latter was to help the sculptor to model a replica that well fitted the face outfit and resulted in optimal adherence of the copy to the tissues, to guarantee both functionality and appearance of the prosthetic nose. To this aim, we designed a process where two physical models of the patient's face are produced. They are different only in the zone of the defect: by means of a simple superposition, they can be used to obtain the positive wax pattern of the nose. This, in turn, represents a realistic model of the shapes and can be used by the sculptor as the initial template to model the prosthetic element (Sansoni et al., 2009a).

To achieve this result, the following steps have been implemented.

2.3.1 Virtual modeling of the defect area

In this step, the whole patient face was acquired by using the Vivid 910 system. To minimize missing data and outliers the TELE lens was used, and full coverage of the face was achieved by acquiring five partial views at maximum resolution (130μm). These views were carefully aligned together by using the *ImAlign* software. Acquisition and alignment were performed in parallel, to guarantee the best quality in the 3D raw data. The time required to complete this step was one hour: in the meantime, the patient was comfortably sitting and relaxed.

The subsequent work was carried out at the laboratory. The aligned point clouds were merged together and, using tessellation, replaced by triangle tessels that maintained the information about the contiguity of the points. This phase was performed by using the *ImMerge* module. The tools available in this software allowed us to trimmer the density of the triangles by adjusting suitable 'tolerance' parameters. In this way it was possible to numerically control the adherence of the model to the original shapes, and, at the same time, to keep the data file as small as possible. The results of this step are shown in Fig. 2. The aligned 3D raw data are presented in Fig. 2.a, and the triangle model of the face is shown in Fig. 2.b.

2.3.2 Virtual modeling of the prosthesis

The aim of this step was to virtually create the nose. To this aim, a number of healthy 'donors' were engaged. The Minolta digitizer was used to acquire the point cloud of their nose at the best resolution. Each point cloud was dragged and matched to the model in Fig. 2.b, to visually appreciate the appearance of the whole face, and to select the most appealing shape from the aesthetical viewpoint. Following the selection the point cloud was elaborated to obtain the triangle mesh, and carefully positioned onto the model in Fig. 2.b. The boundaries were refined and finely blended to the deformity site, to optimize the functionality and the proportions of the prosthesis. The resulting model is shown in Fig. 3.a.

2.3.3 Production of physical prototypes

In this step the two models of Fig. 2.b and Fig. 3.a were extruded. A thickness of 4mm was internally added to the former and externally added to the latter. Fig. 3.b shows both models after the extrusion, along the sagittal median plane: they perfectly match in correspondence with the face regions that are not affected by the deformity. On the other hand, in

correspondence with the deformity, their shape delimits the volume that should be cast by the material used to fabricate the prosthesis.
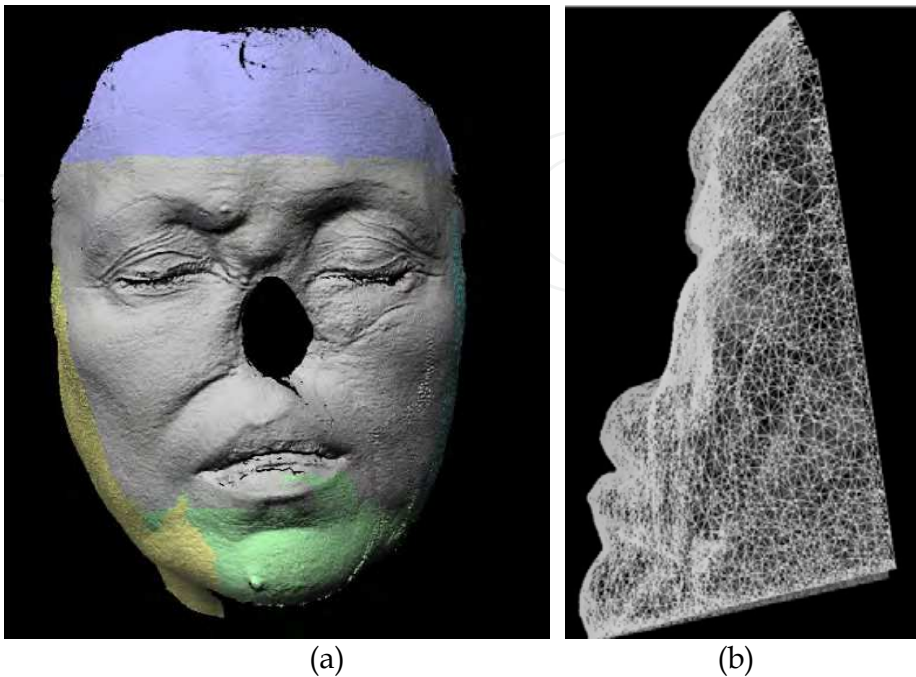

| (a) | (b) |

Fig. 2. Results of the first step. (a): 3D raw data; (b) triangle mesh of the face.
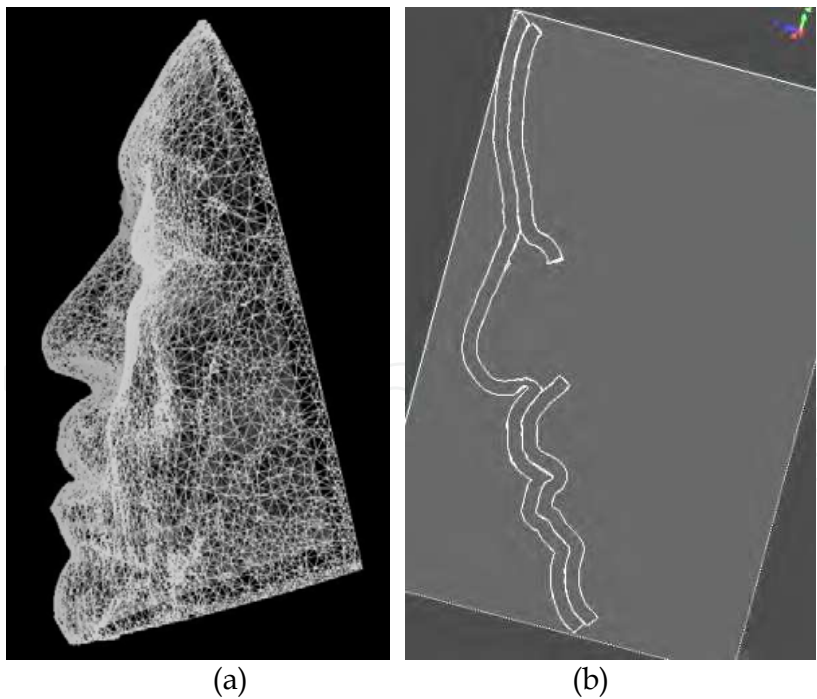

| (a) | (b) |

Fig. 3. Nose addition. (a): Model of the face after the positioning of the nose; (b): Section of the two models along the sagittal, median plane

The triangle mesh of each model was edited and topologically controlled, to produce the STL closed files, used to feed a stereo-lithography machine. The PolyWorks *IMEdit* module

carried out this task. It is a very powerful tool for mesh editing, by means of quasi-automatic transformations (for example, 'fill hole' operations, surface smoothing, triangle optimisation). In addition, it is equipped with specific functions to reliably reconstruct even seriously corrupted portions of the surface.

Following optimization, the meshes were compressed. The PolyWorks *IMCompress* module was used to obtain meshes characterized by lower file dimension, representing an optimal trade-off between accuracy of the representation and memory occupancy.

Then, the STL files were sent through the internet for RP machining. Two physical copies were fabricated using the epoxy photo-polymerizing resin "Somos Watershed 11120" by the SLA 3500 Prototyping Machine. The apparatus is characterized by quite satisfactory tolerances (+/-0.005" for the initial inch, plus an additional 0.0015" for each additional inch), and by reasonable production times. The two physical models are shown in Fig. 4.

2.3.4 Fabrication of the actual prosthesis

In this step, the prosthetic element was fabricated: the two physical models were overlapped to each other and the wax was poured as shown Fig. 5.a. The wax pattern was then extracted from the mould and positioned on the prototype of Fig. 4.a, as shown in Fig. 5.b. In this way, it was possible to perform the try-in of the prosthesis and its refinement on this copy, without disturbing the patient. The definitive prosthesis was obtained by conventional flasking and investing procedures.

Fig. 6 shows the patient's aspect after the positioning of the prosthesis. It was then manually refined to match the skin color and texture.

(a)   (b)

Fig. 4. Physical models obtained by means of rapid prototyping. (a): Model of the original face, internally extruded; (b): Model of the repaired face, externally extruded

2.3.5 Comments

The developed process does not require initial casts and, in principle, it RP machines the physical mould, avoiding fabrication of positive patterns. Hence, the dependence on the anaplasthologist skill is significantly reduced, and the overall process efficiency is increased with respect to traditional approaches. The patient's comfort is optimal, since the acquisition step is quick, contactless and safe. The prosthesis try-in is not necessary and the patient can be involved into the virtual sculpturing of the prosthesis (i.e., the choice of the template

shape and its refinement). This aspect is of primary importance, especially in view of the subsequent replacements of the prostheses, which are necessary due to color changes, aging, contamination and loss of fit.

The production of the physical mould is not expensive (in our case it costed two thousand euros). The method is general: it inherently adapts to the restoration of any other facial defect, with or without symmetrical shapes. For example, it can be fruitfully used whenever the defect involves irregular regions around a single facial organ (i.e., the nose and part of one cheek, the forehead, the orbital and mastoid bone tissues).

(a)   (b)
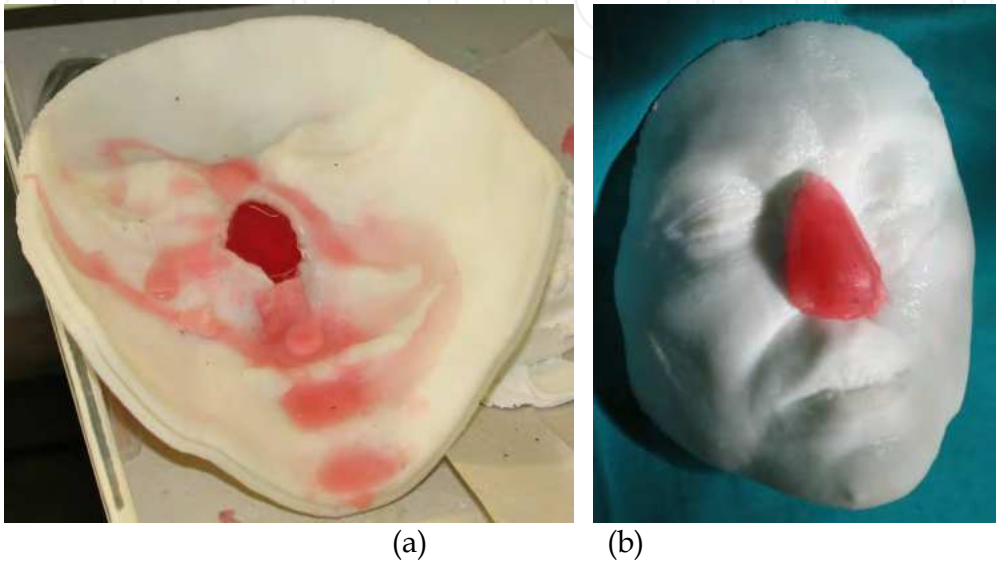
Fig. 5. Fabrication of the wax model. (a): Wax pouring into the cavity corresponding to the defect; (b): superposition of the wax nose onto the physical model of the defect, for further, accurate sculpturing

Fig. 6. Prosthesis of the nose.

2.4 Ear reconstruction

This study case shares the approach based on optical acquisition and modelling of the shapes with the previous one. However, it has been optimized in the prototyping step, since (i) the contralateral organ is available, and (ii) the final prosthesis is directly obtained from the virtual model by means of rapid prototyping.
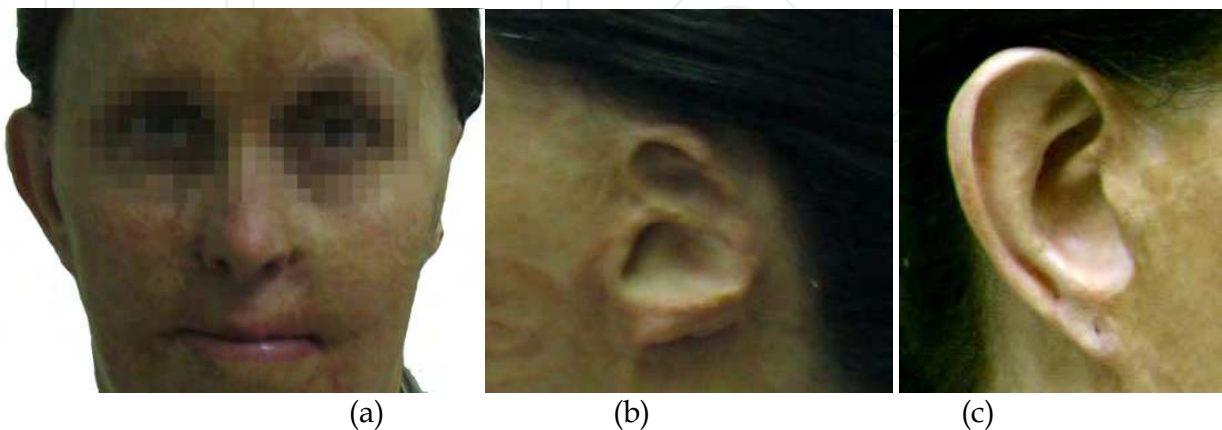
The patient defect is shown in Fig. 7.

| (a) | (b) | (c) |

Fig. 7. Image of the defect. (a): Frontal view; (b) Left ear; (c) Right, safe ear

The left ear was seriously damaged in consequence of a burn. To fabricate the prosthetic element, the right ear, shown in Fig. 7.c was used as the template. The test was performed as follows. Firstly, we acquired the right, safe ear. We configured the Vivid 910 in the MEDIUM mode and acquired four views. Then, the views were aligned and the triangle mesh was obtained and mirrored, in view of using it to model the prosthesis. Fig. 8.a shows the result of the point cloud alignment, Fig. 8.b presents the model of the right ear after mirroring.

Secondly, the defect was gauged. The system configuration was the same as the one in the previous acquisition. Two views were sufficient to cover the whole surface. The mesh was created over the aligned views. The result is presented in Fig. 8.c.

Thirdly, we acquired the whole image patient in the three views shown in Fig. 9. This model was used as the skeleton to align the mesh in Fig. 8.b to the one in Fig. 8.c. The model of the defect was interactively aligned to the skeleton, in order to optimize its position and aesthetical appearance. At this point, the skeleton was discarded. The two models were edited to fill residual holes and to reconstruct missing surface parts (mainly due to undercuts).

Finally, they were finely connected to each other, along their borders. The result of this step is shown in Fig. 10.

The last step was the production of the prosthetic element. The model in Fig. 10 was topologically controlled for the production of the physical copy. The Connex 500 3D Printing System (Objet-Geometries Inc.) was used. This machine is capable of printing parts and assemblies made of multiple polymeric materials all in a single build. The materials used to fabricate the ear prosthetic element were the TangoBlackPlus Shore A85 for the area corresponding to the auricle surface, and the TangoBlackPlus Shore A27 for the areas at the borders of the ear. The former is characterized by higher stiffness with respect to the latter. This technology made it possible to obtain a prosthesis presenting optimal fitting, due to

the use of different materials in the same element. The ear was obtained in about one hour; at the price of 70 €; it is shown in Fig. 11.

(a)   (b)   (c)
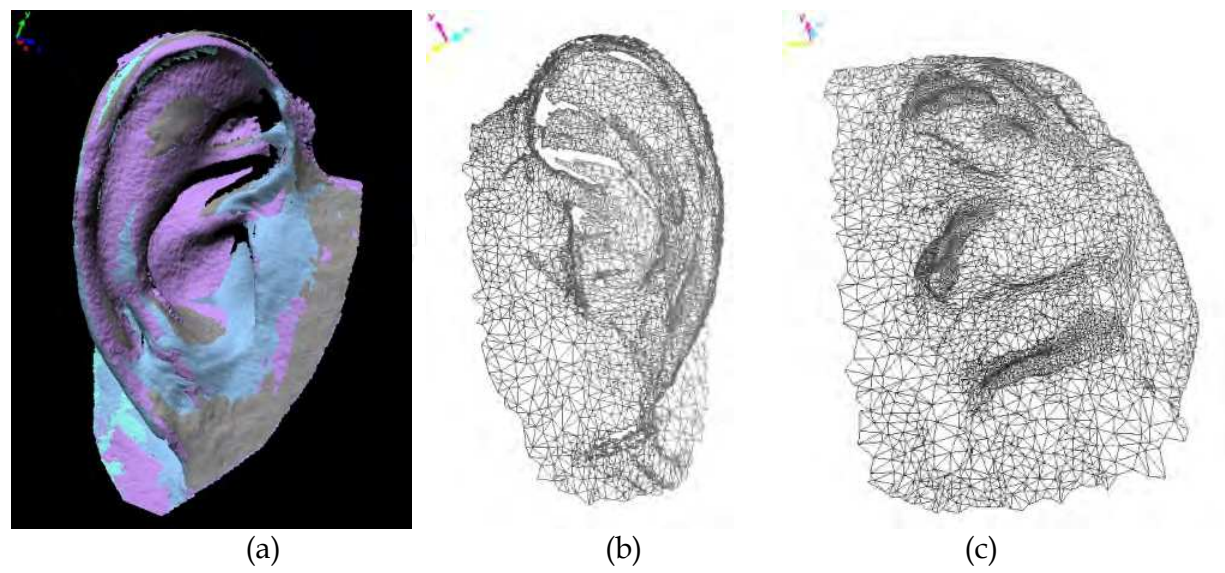
Fig. 8. Acquisition and creation of the ear model. (a): Alignment of the views in correspondence with the right ear; (b): Mirrored mesh of the right ear, (c): Mesh of the defect
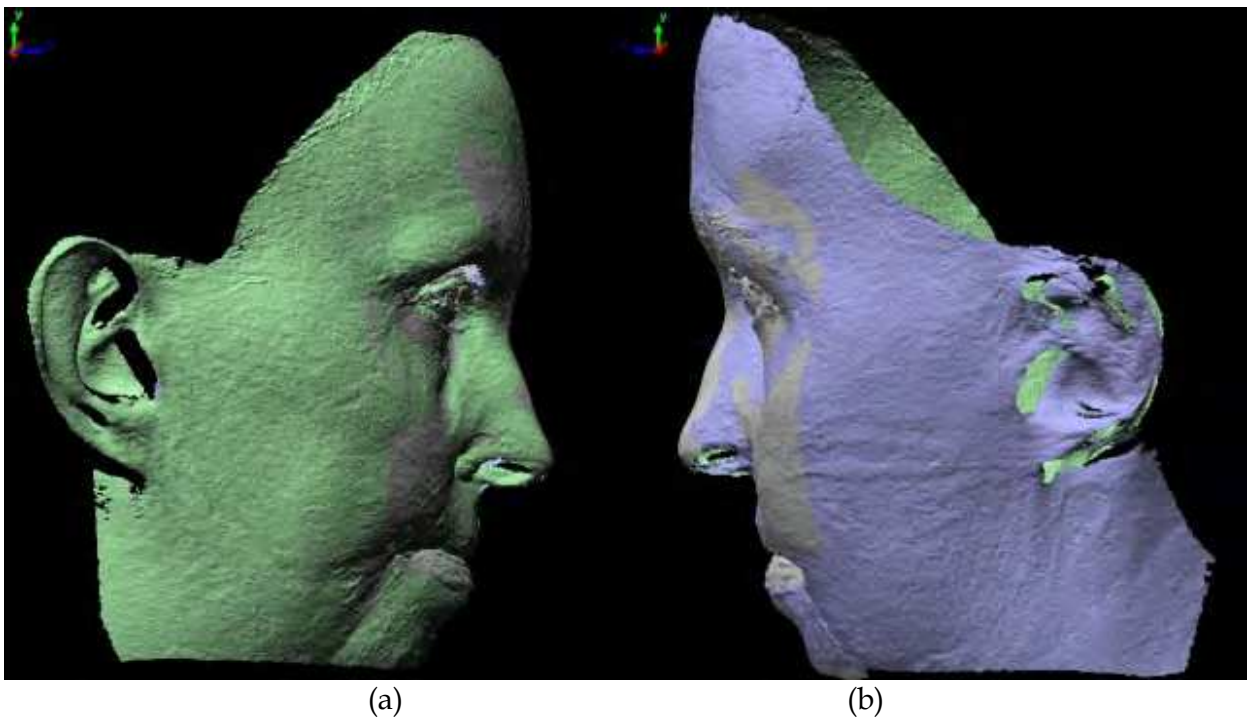

(a)   (b)

Fig. 9. Alignment of the views acquired in correspondence with the face. (a): Right side. (b): Left side

(a)   (b)
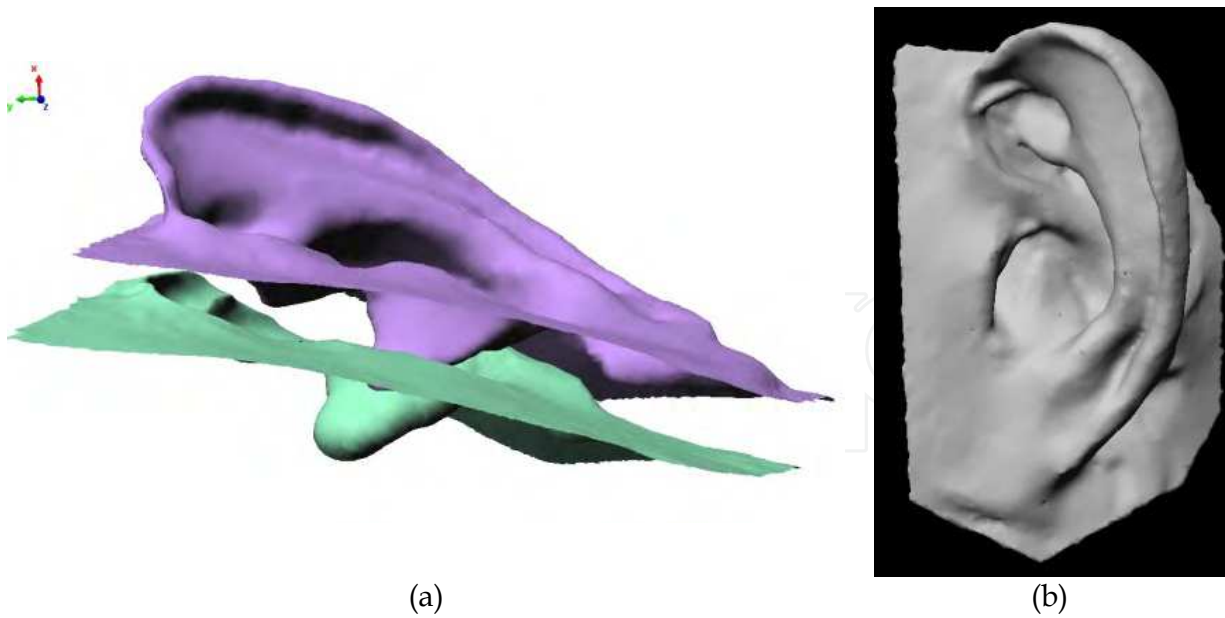
Fig. 10. Final model of the ear prosthesis. (a): Alignment of the models; (b): Front side of the ear model

(a)   (b)
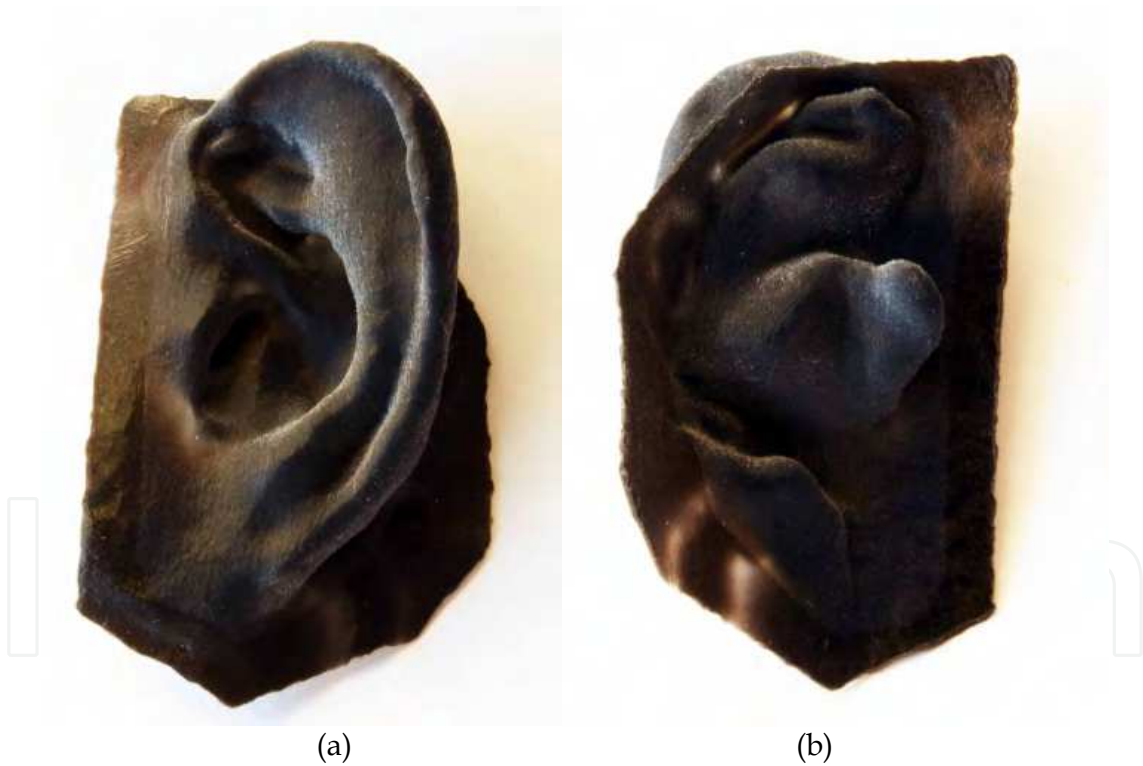
Fig. 11. The final prosthetic element. (a): Front side; (b): Back side

Fig. 12 shows the patient's face after the application of the ear prosthesis. It is worth noting that, in this figure, the ear color was not yet optimized. In fact, we wanted to check its functionality before optimizing it under the aesthetic point of view. We observed optimal quality of the ear shapes, and high adherence to the tissues in proximity of the defect.

As in the previous process, the patient's comfort was optimal, since the acquisition step was quick, contactless and safe. The prosthesis try-in was unnecessary. The prototyping

step was very cheap, the overall time required was about six hours, plus the machining of the prosthesis.

Fig. 12. Application of the prosthetic element to the patient's face

3. The application to forensic medicine

In 2005, the Italian Ministry funded the project entitled "Crime scene: application of optical measurement methodologies for the accurate, contactless acquisition, for the three-dimensional modelling and for the analysis". In this project, we worked together with forensic scientists to provide a full study of body lesions during post-mortem investigation.

Our Laboratory had two objectives. The first was to develop an efficient methodology for the elaboration of acquired 3D raw data, in view of their fruitful analysis and manipulation by operators with minimum computer science training. The second was to provide significant study cases to the specialists, to have their feed-back about both the quality of the measurements and their usefulness with respect to the typology of information and documentation that is currently used for legal purposes.

The main objective of forensic specialists was to learn about 3D optical acquisition, reverse engineering and rapid prototyping, to use these techniques in documenting real crime scenes as well as to study soft tissue lesions, and to produce physical copies of tissues for further analysis (Sansoni et al., 2009b). Production of physical copies is of particular interest to preserve corpse segments that might be used as evidence during subsequent legal judgments, avoiding exhumation. Another application is in the process of identification of unknown victims, when only bones and bone fragments are available.

In this section, the acquisition and the prototyping of a skull are presented. The skull, shown in Fig. 13, was found broken in pieces and brought to the Institute of Legal Medicine of Milan, where the medical examiners managed to reconstruct it, in view of reproducing the face appearance starting from the skull skeleton structure.

Since the skull was really fragile, the risk of breaking it up was high: for this reason, the idea was suggested of "fixing" the tridimensional shape of the skull in a digital archive for futher reproduction in case of need. To acquire the skull, the Vivid 910 optical digitizer was used. It was configured in the MIDDLE setup to capture global views at medium FOV, average resolution, and in the TELE mode to acquire details and fractures.

With the above setup, forty views were acquired, aligned and then fused into the single triangle mesh shown in Fig. 14. This mesh was very detailed, to maintain optimal representation of bone fragments, of teeth and of fractures among the various pieces.
Editing of the mesh was time consuming, since we wanted to reproduce the original shapes as good as possible, especially in regions characterized by very fine 3D edges and details.
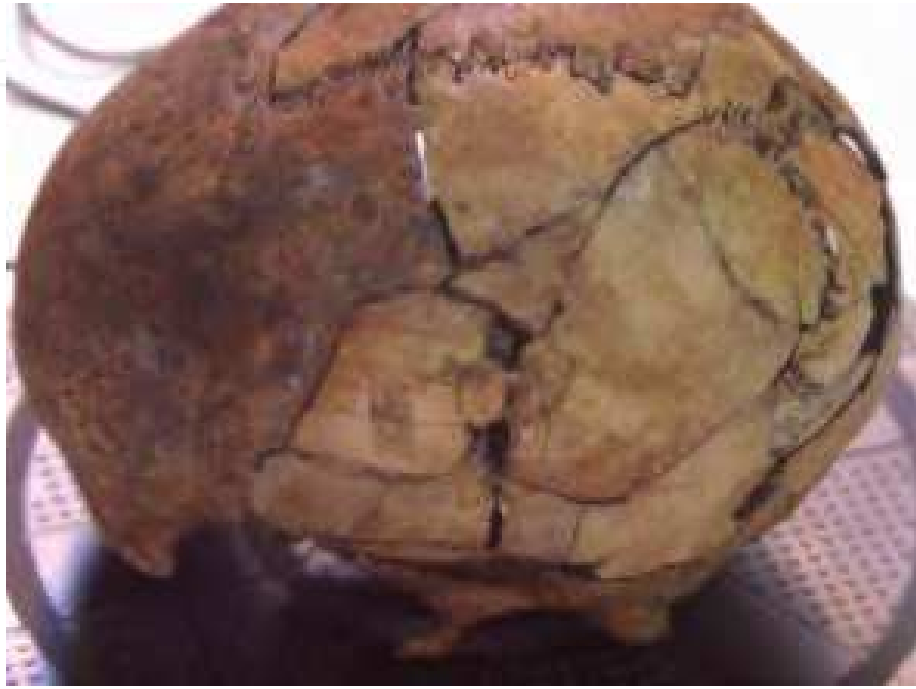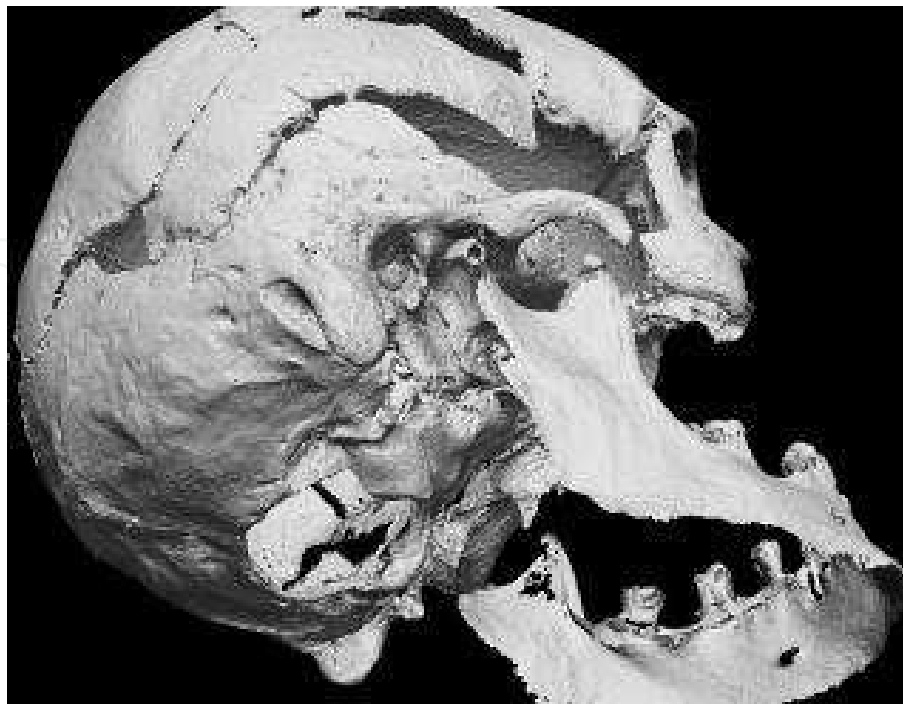

Fig. 13. Image of the skull

Fig. 14. Triangle mesh of the skull

The purpose of this activity was to produce a prototype of the skull, in order to obtain the replica of the find that might be directly inspected by forensic specialists. We achieved this goal: the resulting prototype, shown in Fig. 15, is currently used by the Institute of Legal Medicine of Milan.

Fig. 15. Physical copy of the skull

4. Cultural heritage applications

One of the areas where 3D profilometry is believed to have a bright future is the preservation of cultural heritage through digitization of monuments, buildings, statues, ancient handicrafts, and archaeological findings. Italy is still the repository of more than 80% of the archaeological and cultural heritage of the whole world. As a consequence, it is the natural framework for an intense activity in the field of optical 3D imaging of our heritage. This is achieved thanks to the increasing collaboration with the scientific community in the fields of technology and of cultural heritage. This collaboration meets the favor of Italian institutions, both at the national and the local government levels (Levoy, 1999; Bernardini et al., 2000).

The natural commitment of the Laboratory to applied research and to cooperation with institutions led in 2001 to the establishment of an agreement between the Comune of Brescia and the University of Brescia for the study and the 3D digitization of the statue named "Vittoria Alata" ("Winged Nike of Brescia"), which is located at the Civici Musei di Arte e Storia in Brescia. The initial purpose of the project was to provide archaeologists a sufficient

database that could help them to locate the statue in the correct historical period, and to attribute it to the correct artistic school.

The combined effort of the staff participating to the project, led to the complete digitization of the statue with an overall error of 0.5 mm, to its description in terms of both polygonal and CAD models, and to its reconstruction by means of Rapid Prototyping (Sansoni & Docchio, 2004). The acquisition device used to perform the work is an optical digitizer developed at the Laboratory. It is based on the projection of fringe patterns using incoherent light, and on optical active triangulation (Sansoni et al., 2003).

In this section, we present the results of this activity, that is now completed and has opened exciting perspectives in the collaboration between the Laboratory and the Local (but also others) museums.

4.1 The winged victory of Brescia

The statue is shown in Fig. 16. It is a 2-m bronze statue, found in July 20th, 1826 during the excavations in the large roman Capitolium area of the city. Placing the "Vittoria" in the right temporal and spatial framework is, as strange as it may seem, a metrological problem. A template-matching approach is here involved: the study of the overall proportions of the statue allows the archaeologist, by means of an inductive approach, to determine the archetype from which these proportions have been generated.

Fig. 16. The statue of the Winged Victory located at the City museum

Specialists at the museum were aware that the availability of a set of measurements from a computer-resident replica of the piece, obtained from a high accuracy 3-D digitization of the original artwork, would have been of great help to carry out this study. As a consequence, full 3D digitization of the statue was considered to actively contribute to the verification of the new hypothesis. In addition it was thought strategic to obtain copies of the statue, at different size scales, in view of both didactical and exhibition purposes.

4.1.1 The measuring device

The optical digitizer used to perform the acquisition is shown in Fig. 17.a. The optical head is composed of a microprocessor-controlled Liquid Crystal projector (ABW LCD320) and of a color CCD Camera (Hitachi KP D50), with standard resolution (752x582 pixels). The optical devices are mounted onto a rigid bar, and can be easily moved around the scene by means of a tripod that holds the adjustment units for proper orientation. In essence, the projector projects a sequence of bi-dimensional patterns of incoherent light, according to the well-known Gray Code-Phase Shifting (GCPS) method, upon the object, and the video camera acquires the patterns that are deformed by the object shape (Sansoni et al., 2000).

The system uses suitable calibration and measurement procedures that allow the operator to configure the optical head to work optimally in the operating conditions, depending on the specific levels of environmental light, the surface appearance of the object, and the measurement requirements (i.e., acquisition field, resolution, uncertainty and range). In addition, the device is portable and the optical head can be oriented in the 3D space so that the visibility of the fringes is always optimal, as shown in Fig. 17.b.

(a)   (b)

Fig. 17. The acquisition device. (a): Image of the system; (b): Orientation of the digitizer to optimally view the statue details

4.1.2 Software for point cloud elaboration

The *PolyWorks* suite of programs was selected as the most appropriate to deal with the alignment of so many views, and with the creation and the editing of the statue models.

The alignment module *IMAlign* accomplished the very critical task of registering hundreds of views into a single reference, and of creating a unique point cloud of the whole statue. The modeling of the point cloud was performed in two subsequent steps. The former was the creation of the triangle mesh: the *IMMerge* module of the PolyWorks suite carried it out. The latter was the editing of the mesh: the *IMEdit* tool optimally performed this very complex and time-consuming operation.

The editing step was strategic to obtain an accurate model and to reconstruct even seriously corrupted portions of the surfaces. In addition, the possibility of topologically controlling the triangle mesh was crucial in view of creating a STL closed file to be used by a stereolithography machine.

4.1.3 Acquisition of the point cloud of the statue

The main problem in the digitization of the "Vittoria Alata" was represented by the extension of the surfaces to be measured, considering the height of the statue, and the dimension of the wings. The overall dimension of the statue involved the acquisition of a high number of views (more than 500 in the end) and their alignment.

To minimize the error that inherently accumulates when the views are aligned together, a low-resolution acquisition of the whole statue was performed. A low number of views were taken just before the acquisition of the high-definition set. This data set was efficiently used as a "skeleton", over which the high-definition views were aligned. After its use, the skeleton was eliminated.

To obtain an optimal model in terms of resolution, overall accuracy and file dimension, we used three different set-ups of the system, each one characterized by specific values of measurement resolution and range. These set-ups are shown in Table 2.

	Set-up1 (mm)	Set-up2 (mm)	Set-up3 (mm)
FW x FH	160 x 123	300 x 232	450 x 348
Z-Range	40	100	150
R_z	0.1	0.2	0.3
R_X	0.20	0.38	0.58
R_Y	0.20	0.38	0.58
U_A	0.07	0.09	0.12

Table 2. Geometrical set-ups and measurement performance. FW: width of the Field of View (FOV); FH: height of FOV; Z Range: measurement interval; R_z, R_x and R_Y: average values of measurement and lateral resolutions; U_A: Average value of Type A uncertainties along Z-Range

In the first step, the head of the statue was captured. The digitizer was configured at the highest resolution (Set-up1 in Table 1) and the tripod was elevated up to 3 m above the floor. Fig. 18 shows, as an example of measurement, a particular of the head of the "Vittoria" illuminated by one of the fringe patterns. Fig. 19 illustrates the result of the alignment procedure in the case of the 41 point clouds obtained for the head.

In the second step, the skeleton was acquired with the system configured in Set-up3. 110 point clouds were gauged along predefined directions. These are the 'rings' in Fig. 20 and the vertical stripes in in Fig. 21. Rings are parallel to the basement of the statue, and have been chosen in correspondence with the feet, the left knee and the pelvis of the body respectively. Vertical stripes belong to the front, back, left and right sides of the statue respectively.
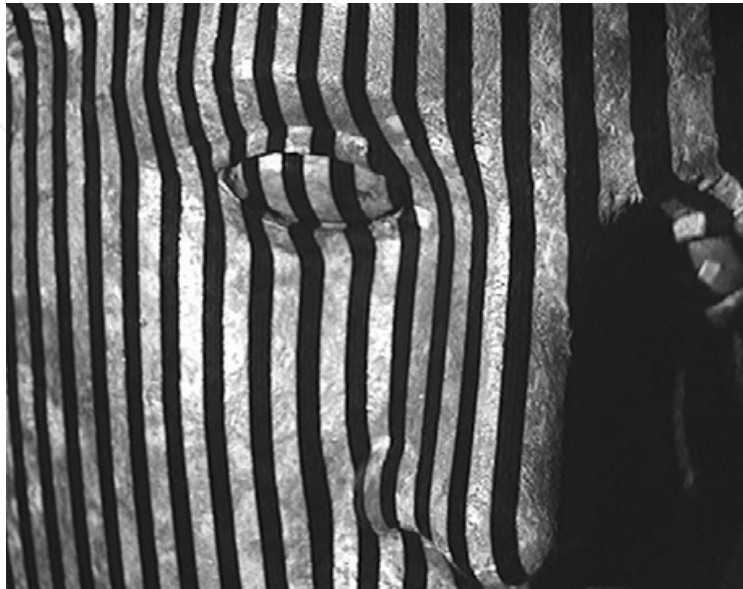

Fig. 18. Projection of a fringe pattern onto the face of the statue

Fig. 19. Multi-view acquisition of the head of the statue (adjacent views are taken with a 40mm overlapping)

In the third step, the accurate high-resolution acquisition of the statue was performed. The optical digitizer was configured in Set-up2. The body of the statue was acquired by turning around the statue with the instrument at different heights. The views were aligned using the skeleton as the reference. Then, the arms and the wings were acquired: the views corresponding to each segment were aligned together, and then registered to the body.

The most important parameters of this step are shown in Table 3. Fig. 22.a shows the result of the alignment of the views, and Fig. 22.b presents the single point cloud obtained by fusing together the partial views. The average measurement error spans from 90μm to 400μm for the 90% of the surface. The maximum error is 1.5 mm in correspondence with the dress folding and the hand-made junctions of the arms and wings.
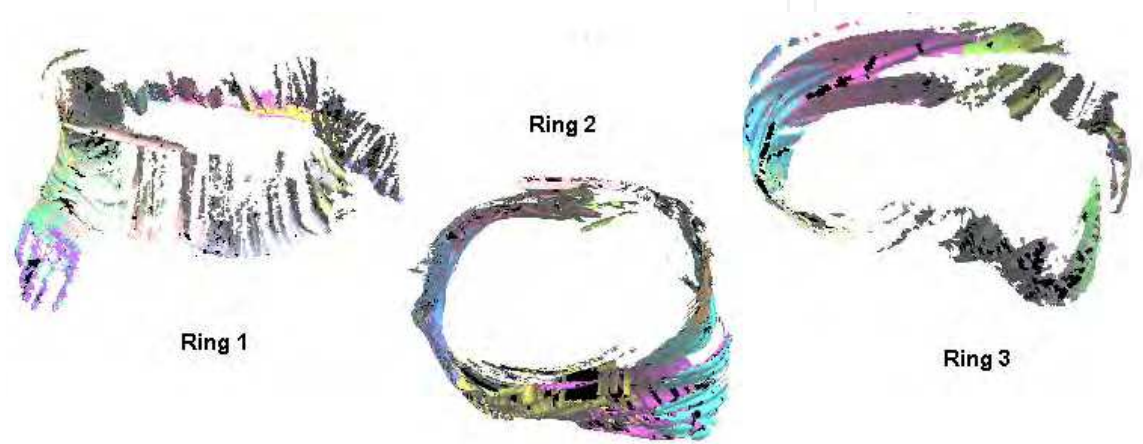
Fig. 20. Rings acquired for the skeleton of the statue

frontal stripe   back stripe   right side   left side

Fig. 21. Stripes acquired for the skeleton of the statue

4.1.4 Generation of the triangle mesh

To fulfil the archaeologist's need to guarantee the highest accuracy for the statue model, we created a very detailed triangle mesh. A good example of the level of detail used to describe the original shapes is the wire-frame representation of the right eye of the head, shown in Fig. 23. The 16-million triangles model, resulting from the editing on the whole mesh is presented in Fig. 24.

	Number of views	% of acquired surface
Head	41	97
Skeleton	110	-
Body	124	93
Arms	62	95
Wings	149	92

Table 3. Parameters of the acquisition

(a)   (b)

Fig. 22. Acquisition of the whole statue. (a): Aligned high-resolution views; (b): Whole point cloud of the statue
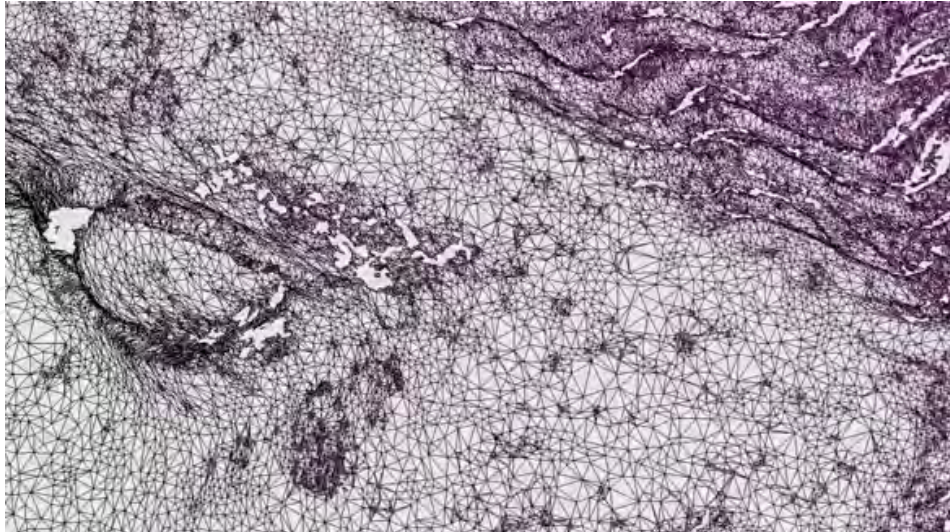
Fig. 23. Wire frame of the right eye of the statue

Fig. 24. Rendered view of the final model of the statue

4.1.5 Applications of the statue model

The availability of the model opened the door to a number of significant applications. Over the years, the specialists have been able to perform their studies on the same model, and this greatly has reduced errors due to subjectivity of interpretation, since they share the same model, and can observe it in great detail, comfortably sit on their chairs. The results are summarized in (Morandini, 2002) where the interested reader can have a comprehensive view of the matter.

Our main interest in the work was the production of a number of models at different compression levels, to be prototyped using stereo-lithography. We worked onto the model of the head of the statue. The work was performed with a collaboration between our Laboratory and the Laboratory of Fast Prototyping of the University of Udine.

A rapid prototyping machine has been used to produce the model, by means of the stereo-lithography technique. The CIBATOOL SL 5190 has been used as the material. The overall dimension of the prototype is 140mm x 110mm x 133mm. The memory occupation of the original STL file was 10MB: it was sent via the Internet to the Laboratory located in Udine. The time required to obtain the copy was 0.2 hours for the elaboration of the data, plus 15 hours for the working of the copy. The prototyped head of the statue is shown in Fig. 25.

We also produced copies of the whole statue: this job was carried out in collaboration with EOS Electro Optical Systems GmbH, located in Munich, Germany. The 30-cm model of the whole statue, shown in Fig. 26, was obtained by compressing the original model to a 3.5 M triangle STL file. This model was input to the EOSINT P 700 laser sintering machine, that machined it in 20 hours. The material used was Nylon P12.

Fig. 25. Physical 1:8 scaled copy of the statue head

In addition, two full scale copies of the statue were machined by the same device. For them, the Laboratory provided the high resolution STL file shown in Fig. 24. This model was segmented into sub-parts, which were separately prototyped. Each part occupied a volume

of 700 x 400 x 600 mm³; the total time necessary to produce all the pieces was 60 hours. Fig. 27 shows the statue conserved at the Civic Museum of Brescia, split into its parts. The other copy is currently placed in the hall of EOS GmbH, as presented in Fig. 28.

5. Conclusions

3D optical acquisition, related instrumentation and elaboration procedures have become valuable tools in support to rapid prototyping. As research and development in the field progresses, more acquisition systems appear in the market able to perform rapid acquisition of moving shapes with in-house calibrated, portable systems.

RP systems will progressively benefit from the availability of these digitizers, closing the loop that links the original physical object shape to the physical replica of the object, in essentially the same way as photography has evolved from the acquisition of the image to its printed form two dimensional replica using high-quality color printers.

Together with 3D television and digital holograpy, rapid prototyping will mark the future of object reconstruction and rendering in virtual and physical spaces.

Fig. 26. Scaled copy of the whole statue (30 cm high)

Fig. 27. The parts of the full scale copy of the statue at the Museums of Brescia

Fig. 28. Copy of the original statue

6. Acknowledgments

7. References

Bernardini, F., Mittleman, J., Rushmeier, H., & Taubin, J. (2000). Building a Digital Model of Michelangelo's Florentine Pietà. *IEEE Computer Graphics and Applications*, Vol.22, No.1, pp. 59-67

Blais, F. (2004). A review of 20 years of range sensors development. *International Journal of Electronic Imaging*; Vol.13, No.1, pp. 231-240

Boulanger, P., Taylor, J., EI-Hakim, S.F., & Rioux, M. (1998). How to virtualize reality: an application to re-creation of world heritage site, *Proceedings of the IV Conference on Virtual Systems and Multimedia*, Gifu, Japan, November 18-20, pp. 39-45

Brasier, S. (1954). *Maxillofacial Laboratory Techniques and Facial Prostheses,* Henry Kimpton, London

Bruschweiler, W., Braun, M., & Dirnhofer, R. (2003). Analysis of patterned injuries and injury-causing instruments with forensic 3D/CAD supported photogrammetry (FPHG): an instruction manual for the documentation process. *Forensic Science International*, Vol.132 , pp. 130–138

Jiao, T., Zhang, F., Huang, X., & Wang, C. (2004). Design and Fabrication of Auricular Prostheses by CAD/CAM System. *International Journal of Prosthodontics*, Vol.17, No.4, pp. 460-463

Levoy, M. (1999). The Digital Michelangelo Project, *Proceedings of 3DIM99, Second International Conference on 3-D Digital Imaging and Modeling*, pp. 2-11, Institute of Electrical and Electronics Engineers, Los Alamitos, USA

Morandini, F. (2002). Rilievo tridimensionale della Vittoria-tavole delle misure, *in Nuove ricerche sul Capitolium di Brescia: scavi, studi e restauri*, pp.165-173

Roberts, A.C. (1971). *Facial Prostheses,* Henry Kimpton, London, United Kingdom

Sansoni, G., Carocci, M., & Rodella, R. (2000). Calibration and performance evaluation of a 3-D imaging sensor based on the projection of structured light. *IEEE Transactions on Instrumentation and Measurement,* Vol.49, No.3, pp. 628-636

Sansoni, G., Patrioli, A., & Docchio, F. (2003). OPL-3D: A novel, portable optical digitizer for fast acquisition of free-form surfaces. *Review of Scientific Instruments,* Vol.74, No.4, pp. 2593-2603

Sansoni, G., & Docchio, F. (2004) Three-dimensional optical measurements and reverse engineering for automotive applications. *Robotics and Computer-Integrated manufacturing*, Vol.20, pp.359-367

Sansoni, G., & Docchio, F. (2005). In-field performance of an optical digitizer for the reverse engineering of free-form surfaces. *International Journal of advanced Manufacturing Technology,* Vol.26, pp.1353-1361

Sansoni, G., & Docchio, F. (2005). 3-D Optical Measurements in the Field of Cultural Heritage: The Case of the Vittoria Alata of Brescia. *IEEE Transactions on Instrumentation and Measurements*, Vol.54, No.1, pp. 359-368

Sansoni, G., Cavagnini, G., Docchio, F., & Gastaldi G. (2009). Virtual and physical prototyping by means of a 3D optical digitizer: application to facial prosthetic reconstruction. *Virtual and Physical Prototyping*, Vol.4, pp. 217-226

Sansoni, G., Cattaneo, C., Trebeschi, M., Gibelli, D., Porta, D., & Picozzi, M. (2009). Feasibility of contactless 3D optical measurement for the analysis of bone and soft tissues lesions: new technologies and perspectives in forensic sciences", *Journal of Forensic Sciences*, Vol.54, No.3, pp. 540-545

Taylor, T.D., (2000). *Clinical maxillofacial prosthetics*, Quintessence Publishing, ISBN 0-86715-391-1, pp. 245-64

Thali, M. J., Braun, M., Bruschweiler, W., & Dirnhofer, R. (2000). Matching tire tracks on the head using forensic photogrammetry. *Forensic Science International,* Vol. 113, pp. 281-28

Thali, M. J., Yen, K., Vock, P., Ozdobac, C., Kneubuehl, B. P., Sonnenschein, & M., Dirnhofer, R. (2003). Image-guided virtual autopsy findings of gunshot victims performed with multi-slice computed tomography (MSCT) magnetic resonance imaging (MRI) and subsequent correlation between radiology and autopsy findings. *Forensic Science International*, Vol.138 , pp. 8–16

Tsuji, M., Noguchi, N., Ihara, K., Yamashita, Y., Shikimori, M., & Goto, M. (2004). Fabrication of a maxillofacial prosthesis using a computer-aided design and manufacturing system. *Journal of Prosthodontics*, Vol.13, pp. 179-83

Modern engineering often deals with customized design that requires easy, low-cost and rapid fabrication. Rapid prototyping (RP) is a popular technology that enables quick and easy fabrication of customized forms/objects directly from computer aided design (CAD) model. The needs for quick product development, decreased time to market, and highly customized and low quantity parts are driving the demand for RP technology. Today, RP technology also known as solid freeform fabrication (SFF) or desktop manufacturing (DM) or layer manufacturing (LM) is regarded as an efficient tool to bring the product concept into the product realization rapidly. Though all the RP technologies are additive they are still different from each other in the way of building layers and/or nature of building materials. This book delivers up-to-date information about RP technology focusing on the overview of the principles, functional requirements, design constraints etc. of specific technology.

INTECH
open science | open minds